PAPER

Millimeter wave control using a plasma filled photonic crystal resonator

IOP Publishing Journal of Physics D: Applied Physics
J. Phys. D: Appl. Phys. **52** (2019) 055202 (6pp) https://doi.org/10.1088/1361-6463/aaee3d

Millimeter wave control using a plasma filled photonic crystal resonator

David R Biggs, Andrea Marcovati and Mark A Cappelli

Mechanical Engineering Department, Stanford University, Stanford, CA 94305, United States of America

E-mail: cap@stanford.edu

Received 30 June 2018, revised 12 October 2018
Accepted for publication 5 November 2018
Published 23 November 2018

Abstract

The manipulation of millimeter-scale microwaves is studied using plasma discharges formed within a vacancy defect of a two-dimensional photonic crystal consisting of a hexagonal lattice of sapphire rods. When an externally driven discharge pulse is generated within the defect, the photonic crystal response is to transmit microwave pulses with variable properties, such as pulse widths and delays as small as 300 ns. Without external drive of the discharge, the device is also shown to behave as a nonlinear power limiter and attenuates the incoming power by 10–15 dB in less than one microsecond when the input power surpasses the threshold of microwave breakdown within the cavity, even at modest incident power of order 1 W. Lastly, by combining external pulse drive with high incident field power but below self-ignition limits, we show using a simple model analysis of the resonator response that the plasma formed spans a wide range of plasma densities, dependent upon the sustaining microwave frequency.

Keywords: plasma, photonic crystal, electromagnetic wave control, mm-wave, pulse modulation

(Some figures may appear in colour only in the online journal)

1. Introduction

Photonic crystals have seen increased applications in the microwave regime during the past few decades. This is particularly true in applications that exploit the stop bands, where strong reflection or attenuation is desired. In a microwave photonic crystal, stop-band attenuation and absorption occurs over a few lattice constants in depth allowing heat to be distributed over a larger volume in comparison to a flat metallic mirror [1]. Photonic crystals have also been used to either guide electromagnetic waves [2] or form resonant cavities for use as accelerators and gyrotrons [3, 4]. Photonic crystals may be made from arrays of either dielectric [5] or metallic [6] rods. Recently there has been an interest in incorporating plasmas as tunable elements in microwave photonic crystals [7], or using high power microwaves with photonic crystal cavities to cause the breakdown of a gas to form a plasma [8–10].

When plasmas are incorporated into microwave devices, the Drude model is often used to describe the plasma as a lossy dielectric, with a relative permittivity ε_p,

$$\varepsilon_p = 1 - \frac{\omega_p^2}{\omega^2 + i\omega\nu_e}, \tag{1}$$

that depends on the wave frequency ω, electron collision frequency ν_e, and the plasma frequency,

$$\omega_p = \sqrt{\frac{e^2 n_e}{m_e \varepsilon_0}}. \tag{2}$$

Here, n_e, e, and m_e represent the electron number density, charge, and mass, and ε_0 is the permittivity of free space. Compared to conventional dielectrics with relative permittivities greater than one that contract wavelengths, plasmas as dielectrics have permittivities always less than one and will expand wavelengths (or negative permittivities that cause waves to become evanescent). In a fixed volume such as a resonant cavity, the introduction of a discharge plasma causes the resonant frequency to increase. By utilizing the ability to control the plasma density by varying discharge properties, we are able to thus introduce tunability or reconfigurability into microwave devices.

Recently, we presented results of studies of a Ku-band microwave resonant cavity that was partially filled with a plasma [11, 12]. The resonant cavity was situated inside a rectangular waveguide section and consisted of two metallic posts that created a volume within which electromagnetic fields were amplified. However, in moving to higher frequencies, such as towards mm-waves (Ka-band or higher), it is advantageous to create resonant cavities using dielectric photonic crystals due to their capability of achieving lower loss and to spread this loss over a large part of the photonic crystal structure. The resonant cavities are formed by introducing a vacancy defect in the crystal lattice.

In this paper, we present an experimental study of a hexagonal lattice photonic crystal with a plasma-filled vacancy defect that resonates in the mm-wave region of the spectrum ($\sim$30 GHz). An hexagonal lattice is used here in these transient investigations, in contrast to the square lattice used in the steady-state experiments of plasma-filled defects presented earlier [7], since a 2D hexagonal lattice affords a higher resonance Q-factor arising from the presence of a complete bandgap (i.e. independent of the wave propagation within the crystal). We show the efficacy of controlling the transmission properties through the crystal using laboratory plasma discharges that alter the permittivity inside the resonant cavity and hence the resonant properties. Furthermore, we demonstrate the multifaceted uses of such a device, including power limiting capabilities due to microwave plasma breakdown and a tunable density plasma source.

2. Methods

The principal device we study in this paper is a photonic crystal with a hexagonal lattice of unpolished sapphire rods of diameter 1.58 mm and a lattice constant of 3.8 mm. This photonic crystal configuration has its first band gap between 25–33 GHz. The crystal is situated inside a hexagonal copper chamber with two WR28 waveguide ports in order to transmit millimeter waves through the device. The chamber was fabricated using additive manufacturing methods with plastics followed by an electroplating process to coat the surface with a conducting layer of 10 μm of copper. We used this same technique on our previous device that consisted of a microwave resonant cavity in a WR62 waveguide [11, 12]. In the hexagonal photonic crystal device we create a resonant cavity by introducing a point defect at the center of the cavity and maintain the same lattice constant at the defect, which results in a resonance frequency of 27 GHz. A photograph of the assembled device, minus the top cover, is shown in figure 1. Last, the device is designed with 1.3 mm access holes situated on top and bottom of the defect in order to have optical access and to allow electrodes to penetrate into the cavity.

The photonic crystal device is dry tested using a vector network analyzer (HP 8722D) for its band gap and defect resonance transmission properties. The resulting transmission versus frequency is shown in figure 2. The left band edge is below the cutoff frequency of the WR28 waveguide and the right band edge is seen at 33 GHz. The band gap has a

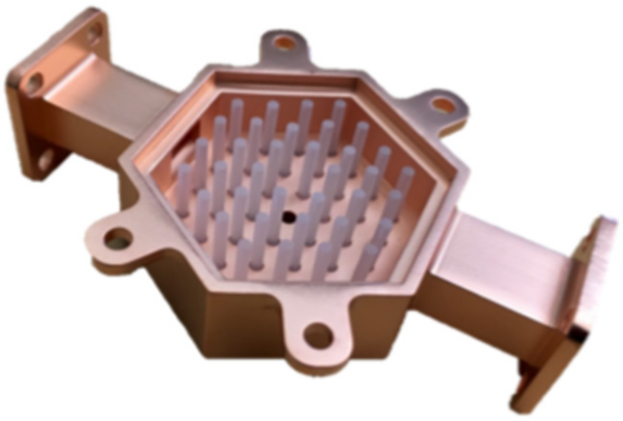

Figure 1. Photograph of a photonic crystal fabricated inside a WR28 waveguide section. The top cover is removed to show the hexagonal lattice of sapphire rods, each 1.58 mm in diameter.

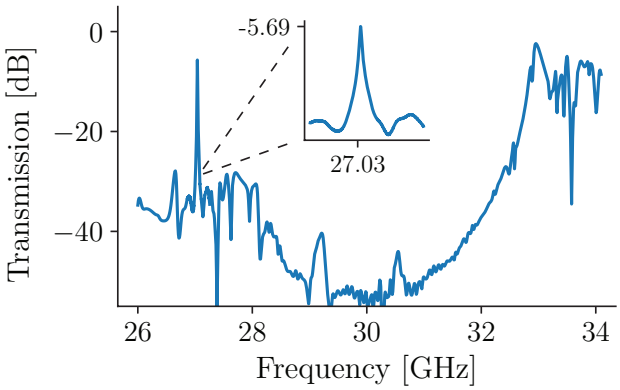

Figure 2. Transmission spectrum through the hexagonal photonic crystal with a defect state at 27 GHz.

maximum depth of 50 dB at its center. The measured quality factor of the unfilled cavity is 4225 and the transmission at resonance is -5.69 dB, both of which well surpass the resonator properties of our previous device.

The experimental setup to introduce plasma into the defect state and measure its modified resonant properties is shown in figure 3; the photonic crystal device is enclosed inside a vacuum chamber that is pumped to low pressures and backfilled with argon gas to 10 Torr. The background pressure is a key parameter in the experiment as it determines the collision and excitation frequency of argon atoms, and hence determines the breakdown condition and resistive losses within the plasma. A more detailed discussion can be seen in [9]. The device is bolted onto a flange with a WR28 waveguide feed-through so that there is very low loss of input power to the device. On the receiving end of the device the microwave signal is picked up by a waveguide to coaxial adapter and the signal is transmitted out of the chamber to a crystal detector using 2.92 mm coaxial cabling.

We transmit either CW or pulsed microwaves using a signal generator (HP 83732A) followed by a frequency doubler (Marki Microwave AQA-2040) and power amplifier (Sage MM SBK-BP273313). A custom high voltage pulse generator from Airity Technologies is used to drive pulsed plasma discharges with tungsten electrodes 0.25 mm in diameter within

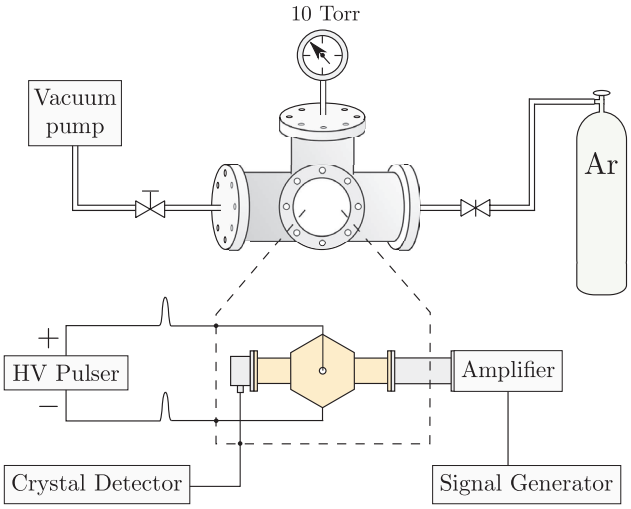

Figure 3. Schematic of the experimental setup to study the photonic crystal device with a combination of microwave electronics, pulsed power supply, and vacuum components. The device is contained within a vacuum chamber and microwave signals are generated, amplified, and passed into the chamber and device through a WR28 waveguide feed-through, before being coupled to a coaxial line and detected by a crystal detector. A high voltage pulsed power supply generates the micro-plasma inside the waveguide using tungsten electrodes.

alumina sleeves that are situated 1 cm apart (the inner height of the cavity). The high voltage pulser is triggered using a Stanford Research Systems Delay Pulse Generator that sends 150 ns TTL pulses at 1 kHz, with resulting voltage and current waveforms shown in figure 4. The leading positive voltage pulse peaks at 1160 V over 150 ns and is followed by a −400 V pulse 275 ns in width. The current pulse has a negative peak of −1.2 A, followed by a positive peak of 0.3 A. Both the voltage and current waveforms have higher frequency ringing not previously seen at lower pressures, and the waveforms are also seemingly chopped off at the peaks, looking more square shaped.

3. Results

We present two sets of experiments, the former using driven electrodes at low microwave powers in order to unobtrusively probe the cavity and study the decoupled behavior, and the latter at high transmission power to study the coupled microwave-plasma behavior.

3.1. Low microwave power experiments

The first set of experiments consist of driving the plasma with the 150 ns, 1160 V pulse shown in figure 4 while transmitting a CW microwave signal. The transmitted power is shown in time for various transmission frequencies, each line corresponding to a trace at a particular frequency shift away from the original 27 GHz ($\Delta f = f - f_0$).

The transmission waveform with a frequency set to 0 Δ f (27.03 GHz) is shown in the dark violet line, and begins at full transmission (0 dB). The plasma ignition causes the

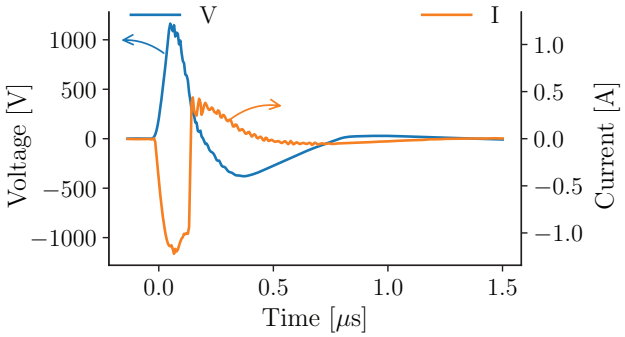

Figure 4. Typical current and voltage waveforms generated while driving a microdischarge in 10 Torr argon with 0.25 mm tungsten electrodes separated by 1 cm.

transmission to drop 20 dB within 1 μs then recover within 75 μs. Compared to our previous work using a simple two copper post resonator in a WR62 waveguide [12], the initial transmission drop occurs in approximately the same time due to a similar voltage pulse waveform, while the recovery is faster by a factor of 5 due to the higher pressure (10 Torr versus 2 Torr). However, it should not be concluded that the WR62 resonator experiments should also be ran at 10 Torr, as such an increase in the pressure would result in a excessively high electron collision frequency, and hence increase in losses within the cavity. It is thus a benefit of the higher frequency of the hexagonal photonic crystal device that we are able to increase the pressure without incurring significant losses.

Increasing the transmission frequency causes the initial and final transmission to decrease in accordance with the unfilled line-shape of the cavity frequency response. It also results in the formation of microwave pulses with delays and widths ranging from tens of microseconds to sub-microseconds. The formation of these tunable microwave pulses has been the motivation of our research in these devices [11, 12], where previously we had achieved in creating microwave pulses at 14 GHz with pulse delays and widths as small as 1 μs and 3 μs, respectively. The microwave pulses are formed when the plasma density changes in time within the resonator, causing a changing plasma-cavity resonance frequency, and hence a CW microwave signal will change from being reflected to transmitted and back to being reflected. The microwave pulses seen in figure 5 occur while the plasma decays, but there should also be microwave pulses due to ionization. However, we see little evidence of microwave pulses due to ionization, likely due to the rapid ionization timescales and the high collisionality of the plasma during this time. It is still clear that setting the transmission frequency to the peak frequency shift of the cavity, around +130 MHz, both ionization and decay of the plasma together cause a single microwave pulse to form with a minimum pulse delay and width of both 330 ns, a substantial improvement over our previous work. However, at larger frequency shifts the attenuation of the microwave pulses becomes greater with 10 dB of loss at the +130 MHz condition. Along with the properties of the microwave pulses formed at small frequency shifts, which can be upwards of 50 μs, the tunable pulse properties of pulse delay and width

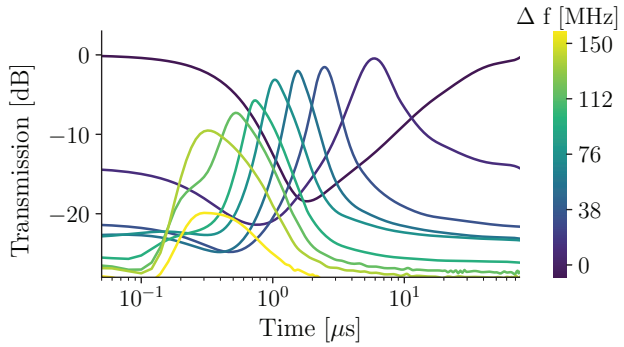

Figure 5. Experimentally measured microwave cavity transmission waveforms for various CW probe signal frequencies, given as $\Delta f = (\omega - \omega_0)/2\pi$ in MHz. The plasma was driven by a voltage pulse shown in figure 4 in 10 Torr of argon.

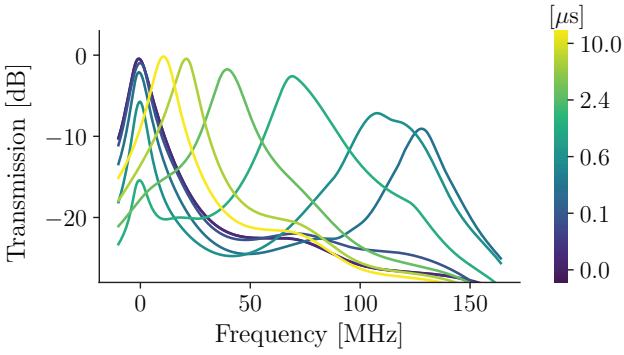

Figure 6. Experimentally measured microwave cavity transmission spectrums at various times during the plasma pulse. The plasma was driven by a voltage pulse shown in figure 4 in 10 Torr of argon.

span over two orders of magnitude with only half a percent change in the transmission frequency.

We also present the same set of microwave data as figure 5 in the frequency domain at various times during the pulse discharge in figure 6. The initial frequency response is a Lorentzian like peak centered at the origin that rapidly moves to +130 MHz in less than 100 ns. The primary resonance at the origin persists for several microseconds, which is consistent with the attenuation slope at low frequency shifts seen in figure 5. Finally, the shifted resonance returns to the origin almost completely in 10 μs.

3.2. High microwave power experiments

We now present experiments that utilized higher microwave power in order to study nonlinear behavior within the photonic crystal cavity. We first study microwave breakdown of plasma inside the cavity by pulsing the input microwave for 5 μs and measuring the transmitted power through the cavity in time. The waveforms of transmitted power in dBm for various input powers to the cavity are shown in figure 7. At input powers below 1.5 W the pulse waveform has a square shape with cavity ring-down occurring after 5 μs. Increasing the power above 1.5 W causes the attenuation mid-pulse due to plasma breakdown and attenuate between 10 and 15 dBm, depending on the input power. Higher input powers also cause

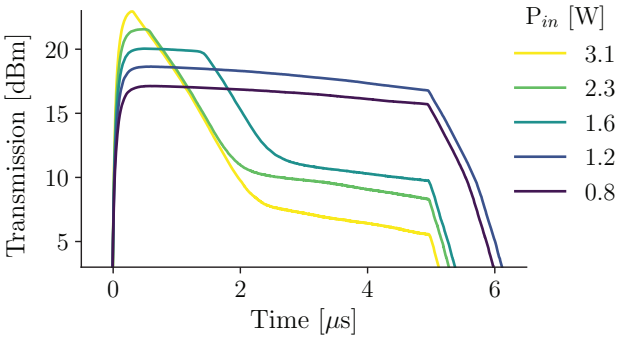

Figure 7. Microwave breakdown during 5 μs high power pulses inside a photonic crystal resonant cavity in 10 Torr of argon.

the plasma to break down sooner, but the decay slope remains relatively constant. This behavior suggests that this sort of photonic crystal device may be used as a nonlinear power limiter, with cutoff powers around 1.5 W. This device is not unique in its power limiting capabilities; there are other devices utilizing plasma breakdown in resonant cavities to achieve similar behavior [8, 10, 13], or thin film devices utilizing semiconductor-metal transitions [14]. However, the benefits of a dielectric photonic crystal over metallic resonant cavity are due to the low loss dielectrics that make possible higher Q devices for lower breakdown powers and lower insertion losses at high frequencies. Finally, utilizing plasma breakdown rather than thin films for power limiting is beneficial because the maximum sustained power will be much higher with the former. Plasmas are self-healing and can absorb more power, increasing plasma density in response, which further detunes the cavity resonance and prevents device failure.

For the last experiment we present, the microwave signal is pulsed for 5 μs at 1.2 W (below breakdown threshold) and simultaneously the high voltage pulse is triggered 500 ns after the microwave pulse has initiated to cause plasma breakdown and alter the transmission properties. The resulting transmitted signal is shown in figure 8, for various transmission frequencies. At Δf = 0 MHz, the microwave signal is simply attenuated over 25 dB in 2.5 μs before plateauing for the duration of the microwave pulse. Higher transmission frequencies have increasing delays in the onset of the microwave pulse since less power is able to transmit away from the unfilled cavity resonance. After 500 ns, these signals rise rapidly before all plateauing at +12 dBm. The cavity is seen to have either an under damped, critically damped, or over damped response depending on the the transmission frequency.

4. Discussion

The low-power microwave pulse data from figure 5 can be also used as a diagnostic of the plasma density resident inside the microwave cavity. There are several ways to do this including electromagnetic simulations [7, 11] and analytic methods [12, 15, 16], with the latter being sufficient for most estimation purposes. We have previously described a theory of plasma density estimation [12], and for convenience to the reader, we repeat the equation for the nondimensional frequency shift

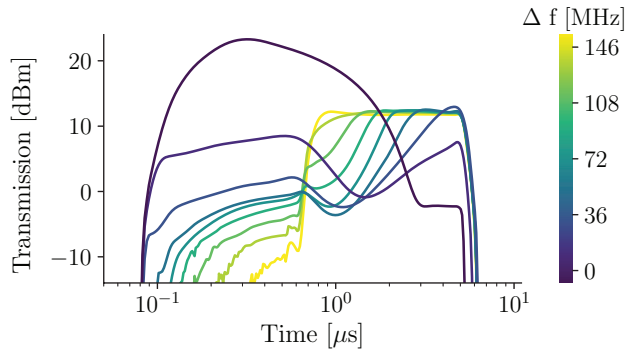

Figure 8. Experimentally measured microwave cavity transmission waveforms for 5 μs high power microwave pulses at various frequencies. A plasma is ignited by a 1160V, 150 ns, pulse in 10 Torr of argon after 500 ns after the microwave pulse begins.

$\Delta\tilde{\omega}_{\rm res} = (\omega_{\rm res} - \omega_0)/\omega_0$, where the subscript 0 denotes the unperturbed properties,

$$\Delta\tilde{\omega}_{\rm res} = \left(1 - \frac{i+1}{Q_0} - \int_V \frac{\omega_{\rm p}^2}{\omega_0^2 + i\nu_{\rm e}\omega_0} E_0^2 dV\right)^{\frac{1}{2}} - 1, \quad (3)$$

that involves a numerical integral about the cavity volume V of the resonant mode profile E_0 weighted by the dielectric response of the plasma. As a simplified analysis, we assume a uniform plasma cylinder with a radius of 1 mm centered inside a cylindrical cavity and solve (3) for various plasma densities. Following this, the inverse problem may be solved to calculate the corresponding plasma density from the measured frequency shift of the cavity. We show both the frequency shift of the cavity and the electron density in time in figure 9(a).

The curve has the characteristic shape consisting of plasma decay due to recombination at early times followed by diffusion at later times. We then estimate the recombination rate coefficient (α) and diffusion timescale (τ) of the plasma by fitting the parameters in the ordinary differential equation,

$$\frac{dn_{\rm e}}{dt} = -\alpha n_{\rm e}^2 - \frac{1}{\tau} n_{\rm e} \quad (4)$$

that has the solution,

$$n_{\rm e}(t) = \left[\frac{1 + n_{\rm e}(t_0)\alpha\tau}{n_{\rm e}(t_0)} \exp\left(\frac{t}{\tau}\right) - \alpha\tau\right]^{-1}. \quad (5)$$

The fitted curve is also shown in figure 9(a) and the normalized residual of the fit is shown in figure 9(b). The fitted parameters are found to be $\alpha = 6.4 \times 10^{-7}$ cm^3 s^{-1} and $\tau = 102$ μs and are similar to previously reported values [11, 17, 18].

We noticed in the last section for the data presented in figure 8 that the transmission plateaued at the same power for a wide range of transmission frequencies, around 100 MHz. In other words, we can say that $T(\omega_1) = T(\omega_2) = $ const., where $\omega_1 < \omega_2$ are transmission frequencies. If we assume that the resonant cavity has a Lorentzian frequency response, then it can be then shown that [19],

$$\left(\frac{\omega_1}{\omega_{\rm res1}} + \frac{\omega_{\rm res1}}{\omega_1}\right)^2 + \left(\frac{1}{Q_1}\right)^2 = \left(\frac{\omega_2}{\omega_{\rm res2}} + \frac{\omega_{\rm res2}}{\omega_2}\right)^2 + \left(\frac{1}{Q_2}\right)^2 = \text{const.} \quad (6)$$

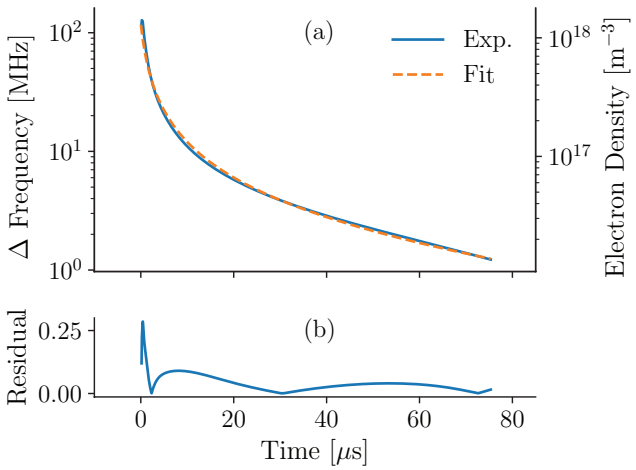

Figure 9. (a) Experimentally measured resonant cavity frequency shift in time is shown as a solid line along with the corresponding plasma density calculated with (3). Also shown in a dashed line is a fit of the parameters in (4). (b) The normalized residual of the ODE fit to the measured electron density in time.

where $\omega_{\rm res1}$ and $\omega_{\rm res2}$ are the shifted resonance frequencies of the cavity with plasma. If we assume that the change in the quality factor of the cavity is small, then given $\omega_1 < \omega_2$ it must be the case that $\omega_{\rm res1} < \omega_{\rm res2}$. Furthermore, if $\omega_1 = \omega_2 + \delta\omega$ then it also must be the case that $\omega_{\rm res1} = \omega_{\rm res2} + \delta\omega$. Thus, since we observed a constant transmitted power across 100 MHz, by (3) this is equivalent to a change of approximately two orders of magnitude in plasma density (from 10^{16} to 10^{18} m^{-3}). This suggests that the sustained plasma density inside the cavity prior to the ending of the microwave pulse is widely variable and dependent upon the small changes in the transmission frequency. This is surprising because with all else being equal, a small frequency change in the transmission frequency should have little to no effect on the electron density. It does in this situation due to increased absorbed power into the plasma, as a result of the permittivity change with the introduction of plasma inside the cavity. In this way, the device seems to act not only as a highly tunable plasma source, but also able to lock into a particular resonant frequency response that is dependent upon the transmission frequency powering the plasma.

5. Conclusion

We have presented in this paper a plasma actuated photonic crystal device with a hexagonal lattice of sapphire rods used to manipulate millimeter-scale electromagnetic waves. By utilizing pulsed plasma discharges, it was shown that microwave pulses of varying properties were produced with widths and delays as low as 300 ns, implying that such devices could be used for modulation or switching purposes with bandwidths upwards of a few MHz. Furthermore, the photonic crystal device was shown to act as a nonlinear power limiter due to microwave plasma breakdown in the presence of high power input microwaves. In this case, microwave pulses were shown to be attenuated between 10–15 dB in 1–2 μs. Last, by

combining both pulsed plasma discharges with high power microwaves, simple model analysis of the experimental results suggest that the resonator cavity served to sustain plasma density tunable over range of values determined by the incident wave frequency. The device used here is constructed using additive manufacturing methods enabling rapid production of practical microwave devices that would have otherwise been difficult or impossible to make by traditional methods.

Future work includes the application of laser or optical diagnostics for independent measurements of properties such as electron density and temperature in order to corroborate our results and findings. The principles of the device studied here, exploiting plasma control of a resonator response, could be applied to microwave couplers, switches, or other forms of junctions.

Acknowledgments

This work was supported by the Air Force Office of Scientific Research (AFOSR) under Award No. FA9550-14-10317 through a Multi-University Research Initiative (MURI) grant titled Plasma-Based Reconfigurable Photonic Crystals and Metamaterials with Dr Mitat Birkan as the program manager.

We would like to thank Dr Luke Raymond at Airity Technologies for his technological support with their high voltage pulser.

ORCID iDs

David R Biggs https://orcid.org/0000-0001-8230-2333
Mark A Cappelli https://orcid.org/0000-0003-3093-3357

References

[1] Brown E R, McMahon O B, Parker C D, Dill C, Agi K and Malloy KJ 1996 Microwave applications of photonic crystals *Photonic Band Gap Materials* (Berlin: Springer) pp 355–75
[2] Jeon S-G, Shin Y-M, Jang K-H, Han S-T, So J-K, Joo Y-D and Park G-S 2007 High order mode formation of externally coupled hybrid photonic-band-gap cavity *Appl. Phys. Lett.* **90** 021112
[3] Shapiro M A, Brown W J, Mastovsky I, Sirigiri J R and Temkin R J 2001 17 GHz photonic band gap cavity with improved input coupling *Phys. Rev. Spec. Top.: Accel. Beams* **4** 042001
[4] Sirigiri J R, Kreischer K E, Machuzak J, Mastovsky I, Shapiro M A and Temkin R J 2001 Photonic-band-gap resonator gyrotron *Phys. Rev. Lett.* **86** 5628
[5] Smith D R, Dalichaouch R, Kroll N, Schultz S, McCall S L and Platzman P M 1993 Photonic band structure and defects in one and two dimensions *J. Opt. Soc. Am.* B **10** 314–21
[6] Smirnova E I, Chen C, Shapiro M A, Sirigiri J R and Temkin R J 2002 Simulation of photonic band gaps in metal rod lattices for microwave applications *J. Appl. Phys.* **91** 960–8
[7] Wang B and Cappelli M A 2015 A tunable microwave plasma photonic crystal filter *Appl. Phys. Lett.* **107** 171107
[8] Parsons S, Gregório J and Hopwood J 2017 Microwave plasma formation within a 2D photonic crystal *Plasma Sources Sci. Technol.* **26** 055002
[9] Gregório J, Parsons S and Hopwood J 2017 Reconfigurable photonic crystal using self-initiated gas breakdown *Plasma Sources Sci. Technol.* **26** 02LT03
[10] Parsons S G and Hopwood J 2017 Millimeter wave plasma formation within a 2D photonic crystal *IEEE Electron Device Lett.* **38** 1602–5
[11] Biggs D R and Cappelli M A 2016 Tunable microwave pulse generation using discharge plasmas *Appl. Phys. Lett.* **109** 124103
[12] Biggs D R, Underwood T C and Cappelli M A 2018 Predictive modeling of plasmas for gaseous plasmonics *Plasma Sources Sci. Technol.* **27** 075005
[13] Semnani A, Macheret S O and Peroulis D 2016 A high-power widely tunable limiter utilizing an evanescent-mode cavity resonator loaded with a gas discharge tube *IEEE Trans. Plasma Sci.* **44** 3271–80
[14] Givernaud J, Crunteanu A, Orlianges J-C, Pothier A, Champeaux C, Catherinot A and Blondy P 2010 Microwave power limiting devices based on the semiconductor–metal transition in vanadium–dioxide thin films *IEEE Trans. Microw. Theory Tech.* **58** 2352–61
[15] Rose D J and Brown S C 1952 Methods of measuring the properties of ionized gases at high frequencies. III. Measurement of discharge admittance and electron density *J. Appl. Phys.* **23** 1028–32
[16] Crawford F W, Kino G S, Self S A and Spalter J 1963 A microwave method for the study of steady and fluctuating plasma number densities *J. Appl. Phys.* **34** 2186–96
[17] Shiu Y-J and Biondi M A 1978 Dissociative recombination in argon: dependence of the total rate coefficient and excited-state production on electron temperature *Phys. Rev.* A **17** 868
[18] Sergeichev K F, Lukina N A and Fesenko A A 2013 Long-lived ar-hg plasma in the afterglow of a high-current pulsed discharge *Plasma Phys. Rep.* **39** 144–54
[19] Slater J C 1946 Microwave electronics *Rev. Mod. Phys.* **18** 441